ELECTRON CONFINEMENT AND SINGLE ELECTRON EFFECTS IN METALLIC AND SEMICONDUCTING NANO-CLUSTERS

Leonid Gurevich, Luca Canali, and Leo P. Kouwenhoven
Quantum Transport Group and DIMES,
Delft University of Technology, PO Box 5046, 2600 GA Delft, The Netherlands
Erik P.A.M. Bakkers and Daniel Vanmaekelbergh
Debye Institute, University of Utrecht, P.O. Box 80000, 3508 TA Utrecht, The Netherlands

ABSTRACT

We review our recent transport measurements on metallic (Au, Pt, Pd) and semiconducting (CdSe) nanoclusters using low-temperature scanning tunneling microscopy (STM). We have developed special tips for STM containing both a tunneling tip as well as a gate electrode. This allows field-effect measurements on arbitrary nanoclusters.

1. INTRODUCTION

Transport measurements on small particles reveal interesting deviations from bulk properties. In this paper we concentrate on two physical phenomena: Coulomb blockade and quantum confinement. The former one is determined by the capacitance between the particle and the environment and therefore depends on the size of the particle and measurement geometry (i.e. vicinity of the contacts). A basic explanation of Coulomb blockade can be illustrated by considering that the energy necessary to put a charge q on a conductor of capacitance C, is $q^2/2C$. The capacitance scales as the size of the conductor and, thus, the charging energy increases as $1/r$ when the size of the conductor decreases. Moreover, the total charge of an isolated metallic cluster has to be an integer multiple of the electron charge e, so that there is a minimum energy which the electrons must have in order to be able to jump onto the cluster from the contact leads. This is the single electron charging energy $E_C = e^2/2C$. For example, the energy to put one electron into a cluster with diameter ~1 nm is of the order 1 eV. When $E_C > k_BT$ this effect can manifest itself in the I-V characteristic as a blockade of the current. For a quantitative explanation of Coulomb blockade phenomenon we refer to the theory of single electron charging effects developed by Averin, Likharev, and Korotkov and also by Beenakker (see, for example, Ref. 1). The quantum confinement effects can be observed when the diameter of the particle is of the same order of magnitude as the wavelength of the electron wavefunctions. In that case the energy spectrum changes from continuous to discrete [2]. In the simplest model a nanocrystal can be considered as an “electron box” where energy levels are the solutions of the Schrodinger equation for the box of given size and geometry. Better qualitative agreement with experiment can be obtained if the chemical composition of the nanocluster is taken into account [3]. To get the complete picture of the electron energy levels in a nanocluster scattering of the electrons inside the clusters, influence of the surface states and ligand groups should also be considered.

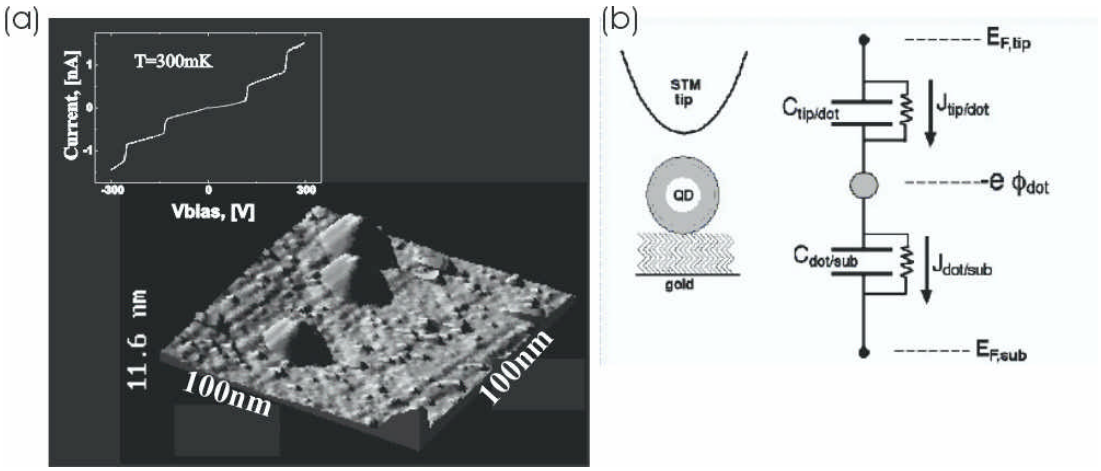

Fig.1 (a) STM topography image of the 5nm Au clusters deposited on the flame annealed gold substrate. 4-Aminothiophenol has been used to anchor the clusters. The insert shows a typical I-V curve measured on top of a cluster. (b) Schematic of the scanning tunneling spectroscopy experiment on a nanocluster. Double barrier tunnel junction is formed by the STM tip, cluster and substrate. The tunnel barrier between the cluster and the substrate is provided by an insulating self-assembled monolayer.

Although several successful measurements on metallic and semiconducting particles have been published [4,5,8-11] the issue of preparing stable contacts to the nanoparticle remains unsolved. There are two main experimental approaches to the problem, each with their advantages and drawbacks. On one hand, Scanning Tunneling Microscopy (STM) proves to be a versatile tool for fundamental studies of single-electron transport through the nanocrystals [4, 5, 6]. The nanocrystals immobilized on the conducting surface can be located by the STM in topography mode (Fig. 1a). Afterwards the tip is positioned above the dot, thus forming a substrate/dot/tip Double Barrier Tunnel Junction (DBTJ) (Fig.1b). In a typical experiment the tunneling current I is measured as a function of the bias voltage V across the junction. Assuming a flat density of states in the tip and the substrate, peaks in the dI/dV versus V will correspond to the opening of resonant tunneling paths via the energy levels in the dot. Besides the ability to locate and image clusters, STM offers the possibility to tune the properties of a DBTJ by changing the distance between the tip and cluster [7] thereby changing the resistance (and to lesser extent the capacitance) of the tip/cluster junction. As we will demonstrate below, this allows to tune relative tunnel rates from the tip to the cluster and from the cluster to the substrate and hence to control the electron occupancy of the dot.
Until recently STM spectroscopy was limited to two-terminal measurements. An additional gate electrode gives control over the electrostatic potential of the nanocluster and therefore the electron occupancy can be changed while keeping the bias voltage small. We will describe an experiment involving 3-terminal STM spectroscopy on a 20 nm gold cluster [8].
On the other hand, the nanocluster can be attached between two fixed electrodes [9,10,11] or even prepared between them [12]. This approach has an advantage of improved junction stability and therefore, at least in theory, can provide better energy resolution.

2. SCANNING TUNNELING SPECTROSCOPY (STS) ON SEMICONDUCTING AND METALLIC NANOCLUSTERS

We start with a discussion of our low-temperature STS experiment on 4-nm CdSe clusters. We measure the dI/dV spectra of the clusters in a double-barrier geometry for the case of symmetric and asymmetric junctions. The different symmetries of the barriers mean different occupations of the electrons inside the clusters, which we observe to have profound effects in the tunneling spectra.
We prepare our sample by depositing CdSe clusters on a flat Au substrate. A trioctylphosphineoxide (TOPO) capped CdSe clusters have been synthesized according to the procedure described in Ref. 13 and deposited from suspension onto a flame annealed gold substrate covered with cyclohexylidene self-assembled monolayer (SAM). The cyclohexylidene SAM fixes clusters on the surface and provides together with the capping layer the tunnel barrier between the cluster and the substrate.
Imaging and spectroscopy was performed using home-built low-temperature STM [14] at 4.2K. Figure 2 shows an STM image of one of our samples. The triangular structures in the topography are atomically flat

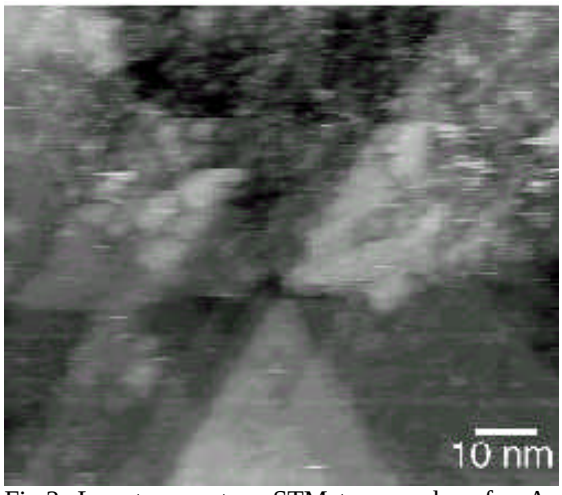

Fig.2. Low-temperature STM topography of a Au (111) substrate covered with a submonolayer of CdSe clusters.

terraces from the flame annealed gold substrate. On top of that we can see a sub-monolayer of nanoparticles. After imaging we position the STM tip on top of an isolated dot to acquire its spectroscopic characteristic. We have recorded tunneling spectra on several dots for various tip-to-dot distances between 0.5 nm and 1.6 nm (estimated from the junction resistance).

A typical tunneling spectrum obtained at large distance (~1.6 nm) is shown on Figure 3a. Under these conditions the cluster oscillates between the states with 0 and 1 extra electron at positive bias, when tunneling via the conduction band (CB) occurs, and states with 0 and –1 extra electron at negative bias (tunneling via valence band, VB). The probability to find more than one extra electron on the dot is very low in this case (i.e. tunneling off is much faster than tunneling into the cluster) and therefore peaks in dI/dV correspond to tunneling through single particle orbitals. The averaged peak spacings obtained using the spectra of ten 4.3 nm CdSe clusters are: $DV_{1\text{-}2}$ =190 meV, $DV_{2\text{-}3}$= 195 meV, $DV_{3\text{-}4}$=150 meV, and $DV_{4\text{-}5}$= 92 meV, (±15 meV). The zero conductivity gap (between –1.6 V and +1 V) corresponds to HOMO-LUMO gap of the 4.3 nm CdSe cluster plus the charging energy necessary for creation of an extra electron and hole. All these values agree fairly well with the pseudopotential calculations* [3,7]. We note that the increase in peak intensity with increasing bias may be explained by an increased spatial extent of the states with higher momentum.

When the tip-cluster distance decreases the mean electron occupancy of the dot increases. Now charging effects become important since electron accumulate on the cluster. As shown in figure 3b, in the spectrum obtained at 0.55 nm tip-cluster separation the first peak (corresponding to the tunneling into an s-wave orbital) splits into a doublet. The second one (p-orbital) splits into a sextet. The separation between the satellites stays more-or-less constant; it is equal to the charging energy of the dot e^2/C. We like to

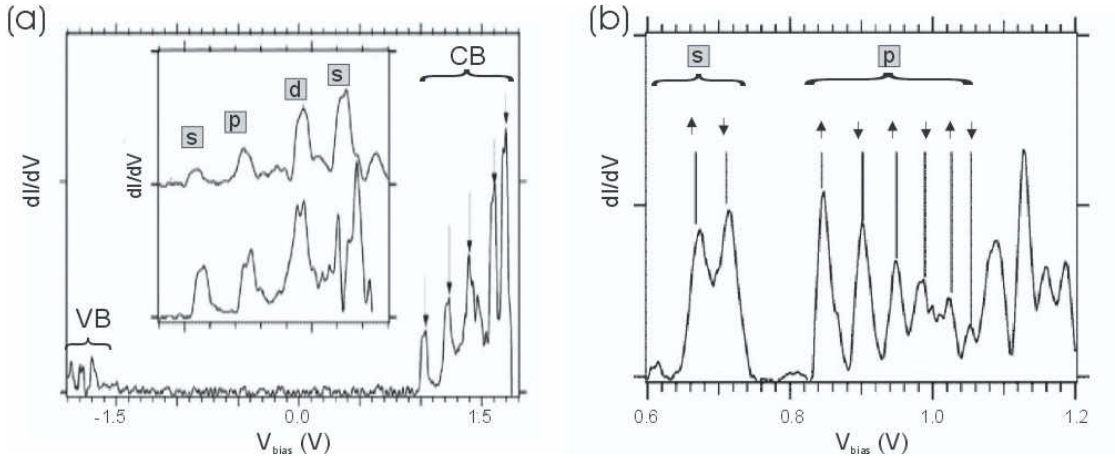

Fig.3 Tunneling spectra obtained on a 4.3 nm CdSe dot, T=4.2K. (a) Set point 5pA at 1.4V (estimated tip/dot distance – 1.6nm). Tunneling spectrum corresponds to single particle spectrum and the peaks can be identified as tunneling into s,p,d and s orbitals, correspondingly. The insert shows spectra obtained on two other dots. (b) Set point 80pA at 1.5V. Peaks are split with the spacing corresponding to the charging energy.

* In the experiment the bias voltage is divided between tip/cluster and cluster/substrates junctions according to their relative capacitance. As we will show in the next section, even in a case of the cysteamine SAM (the shortest molecules used), 80% of the voltage drops between tip and cluster. For simplicity, we will therefore translate 1mV of bias into 1meV of electron energy.

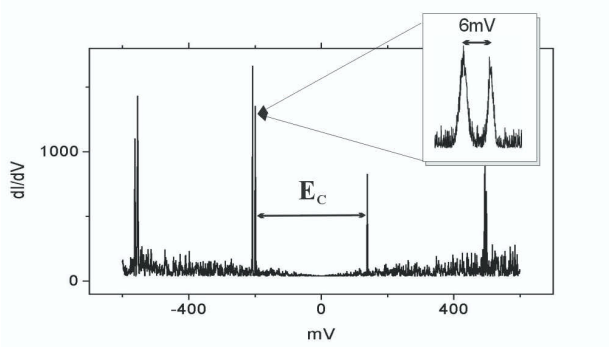

Fig. 4. Tunneling spectrum taken at 300 mK on top of a 4 nm Pd cluster deposited on flame-annealed gold substrate covered with 4-aminothiophenol SAM. The insert shows splitting of the peaks caused by discrete electron energy levels in the metal cluster.

emphasize here that the charging energy is smaller than the spacing between the single-particle states (i.e. the s- and p-states). This is in the contrast to the microfabricated quantum dots with sizes in the range of 100nm or more where the charging energy is usually an order of magnitude larger than the level separation [15].

The situation is different in metallic clusters where single particle states are much more difficult to resolve. Due to higher electron density the level separation is much smaller (mean level separation $\varepsilon \sim E_f/N$, where E_f – Fermi energy and N – number of electrons) and in practical cases it is significantly smaller than the charging energy. For example, for 4 nm gold particle the mean energy level separation is expected to be about 1 meV, while the charging energy is about 100 meV. In this situation the energy levels should be observed as sub-steps on the Coulomb staircase (in an I versus V graph) or closely separated satellite peaks on dI/dV versus V plot. A spectroscopy curve (dI/dV) taken on top of a 4 nm Pd cluster is shown in figure 4. We indeed observe splitting of the peaks that can be attributed to discrete electron energy levels of the metal cluster. However, smearing of the peaks prevents us from studying details. While the energy resolution of our system at this temperature is below 1K (~0.1 meV), we observe a peak width of about ~1 meV. This is presumably caused by the instability (vibration) of the tip-cluster junction. Combined X, Y, Z vibrations as small as 0.03 nm can cause the observed peak widening[1]. The problem may be solved by using a fixed electrode arrangement.

Summarizing, we have shown that in STM spectroscopy on semiconductor nanoclusters charging effects can be switched "on" and "off" by varying the tip/cluster separation. At large tip/cluster distances a single-particle spectrum can be obtained. Resolution of discrete energy levels in metal clusters is limited by tip-cluster instabilities.

3. SCANNING GATE SPECTROSCOPY ON NANOCLUSTERS

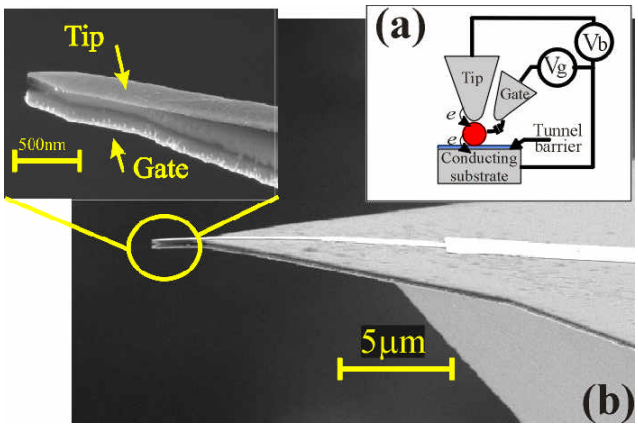

FIG.5. (a) Scheme of the scanning gate probe. The STM tip is positioned above a metallic cluster (represented as a sphere). An electron coming from the tip will first tunnel onto the cluster and then tunnel into the conducting substrate. A gate electrode can be used to change the offset charge of the cluster, thus forming a system equivalent to a single-electron transistor. (b) SEM image of a scanning gate probe. Metal electrodes are deposited on the two sides of a SiN_x-SiO_2-SiN_x cantilever. The separation between the electrodes is about of 200 nm and the typical radius of curvature of the sharp end of the tip is approximately 30 nm.

So far, a gate electrode has been absent in all STM studies. In this chapter we describe the design and operation of a scanning probe, which extends normal STM capabilities by means of an extra gate electrode. The probe enables to acquire three-terminal spectroscopic characteristics of nanostructures deposited on a conducting surface. The gate can also be used to avoid the extra level smearing caused by high bias voltages and currents, by shifting the electronic levels in the nanostructure towards the Fermi energy of the leads. Three-terminal electrical measurements have already been proven very fruitful in the field of SET transistors and semiconductor quantum dots [15].

We microfabricate the scanning gate probes using a multilayer

[1] Indeed, the tip vibration δz translates into the uncertainty of the charge induced on the cluster: $\delta q \sim VC(\delta z/z)$, which in turn leads to the energy uncertainty (peak widening) $d\varepsilon \sim e\,\delta q/C$, where V – bias voltage, C – tip-cluster capacitance and e – electron charge.

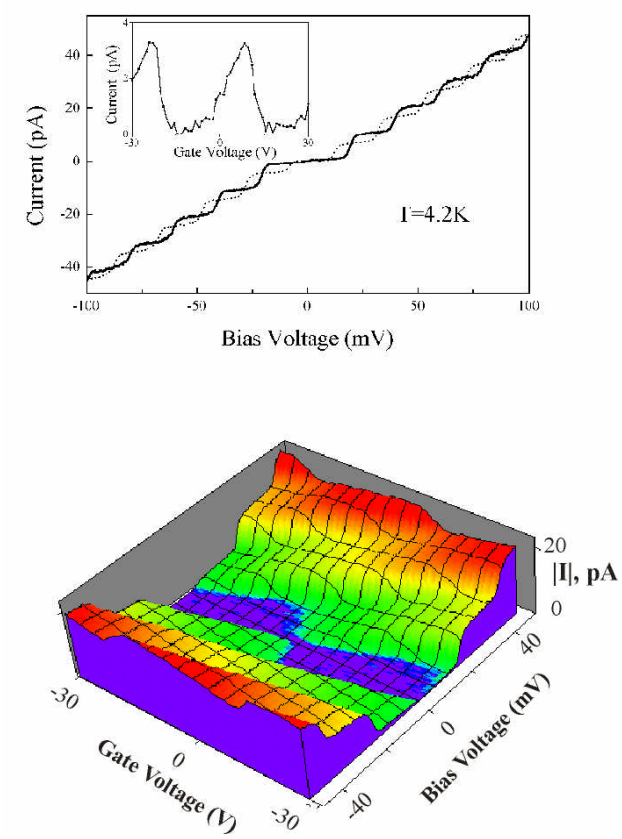

FIG. 6. Scanning gate spectroscopy of a 20-nm Au cluster at 4.2 K. Top graph: *I-V* curves taken with the scanning gate tip positioned on top of a cluster for two different gate voltages V_g = -2.4 and 15.6 V, corresponding to an induced charge on the cluster Q_0 = 0 and $e/2$ respectively. Inset: Current versus gate voltage characteristic with bias voltage V_b = 8.4 mV. Lower image: Complete set of I-V curves represented as a three-dimensional plot.
The barrier capacitances and resistances estimated from the data are: $C_1 = 8\times10^{-18}$ F, $C_2 = 1\times10^{-18}$ F, $C_g = 5\times10^{-21}$ F, R_1 = 2 GΩ, R_2 = 50 MΩ, where C_1 and R_1 refer to the tip-cluster barrier, C_2 and R_2 refer to the cluster-substrate barrier and C_a is the gate-cluster capacitance.

process involving e-beam and optical lithography [8]. The probes consist of two closely separated metal electrodes (with a distance of about 200 nm) extending onto the sharp ends of a silicon nitride cantilever (Fig.3b). Etched groove between the electrodes provides good electrical isolation: up to 70V can be applied between the electrodes before leakage current (>1 pA) is detected. The whole chip has a size similar to commercial tips used for atomic force microscopy (AFM) ~ 2 x 4 x 0.5 mm^3. They are easy to handle and can be installed in standard STM heads.

We demonstrate the functioning of the scanning gate probes by performing spectroscopic measurements on a test sample consisting of 20-nm gold clusters deposited on a flat platinum film. The sample is prepared taking into account the following constraints. The clusters have to be fixed on the surface during scanning and spectroscopic measurements. There must be an insulating layer between the clusters and the metal substrate to provide a tunnel-barrier. The insulator must have a smooth *I-V* characteristic in the bias window of interest for spectroscopy on nanoclusters (about 1 V). Finally, the clusters must be well separated from each other, otherwise their capacitive coupling to the gate would be reduced and some parasitic potential jumps caused by moving electrons in the neighbouring clusters might occur. These requirements are fulfilled by depositing 20-nm gold colloids [16] from a charge-stabilised aqueous solution onto a Pt substrate covered by a self-assembled monolayer of cysteamine. This monolayer both bonds the colloids to the substrate and forms the tunnel barrier between the clusters and the Pt film. The density of the clusters absorbed on the surface was tuned to the optimal value (10 - 100 μm^{-2}) by changing concentration and incubation time in the colloidal solutions. STM topographies are acquired with a relatively high tunnel resistance (and thus large tip-sample distance) of the order of 10 GΩ, to prevent the clusters from moving on the surface. From the topographic images we find the position of the gold clusters so that we can position the scanning gate on top of one of them and measure its *I-V* characteristic.

Figure 6 (top graph) shows two such *I-V*s obtained for different gate voltages, corresponding to an offset charge on the cluster Q_0 = 0 and e/2. Coulomb charging steps are clearly visible, with a step size of about 15 meV (as expected for 20-nm metallic clusters). We acquired a set of 50 *I-V*s for different gate voltages varying from -30 V to +30 V using the STM program. Before each *I-V* curve, the STM tip is stabilized by the feedback loop with bias voltage V_b = 100 mV, tunnel current I_T = 50 pA and gate voltage V_g = 0. Then the feedback loop is turned off and the gate voltage is swept to the intended value. Afterwards we acquire the *I-V* data points, sweep the gate back to zero and turn the feedback on again to stabilize the STM tip.

The measurements are shown as a three-dimensional plot in Fig. 6. Such a figure is called the stability diagram of a single-electron transistor [17]. The dark area at the centre of the image corresponds to the Coulomb blockade of transport: the current through the cluster is blocked because the electrons in the leads do not have enough energy to tunnel onto the cluster (their energy is lower than the charging energy of the cluster). Areas represented with different shades correspond to processes where one or more electrons can tunnel simultaneously through. The discrete electronic spectrum of the cluster could not be resolved, as expected, since the mean electron-level separation for a 20-nm cluster can be estimated to be less than 1 K. Using the *orthodox theory* of single electron tunnelling we were able to calculate the values for the capacitances and resistances of the tunnel barriers and for the gate capacitance (see the caption of

Fig. 4).

In conclusion, we have developed a scanning gate probe for studying nanostructures such as molecules and metallic clusters. The probe can image and perform three-terminal spectroscopy on nanostructures deposited on a conducting substrate.

ACKNOWLEDGEMENTS

We would like to thank Martin Upward for the help with the low-temperature measurements in the dilution fridge, Hugo de Wit for the help at the early stages of the work, Michael Janus, Yann Kervennic, Michel Hendriks, Herre van der Zant and Danny Porath for discussions. The authors gratefully acknowledge funding for this work by FOM (Dutch Stichting voor Fundamenteel Onderzoek der Materie) and ERATO (Exploratory Research for Advanced Technology).

---

1 D.V. Averin and K.K. Likharev, Mesoscopic Phenomena in Solids, edited by B.L. Altshuler, P.A. Lee and R.A. Webb et al. (Elsevier, Amsterda, 1991), p.169.
2 A.P. Alivisatos, Science **271**, 933 (1996).
3 A. Franceschetti and A. Zunger, Phys.Rev.B **62**, 2614 (2000).
4 M. Dorogi, J. Gomez, R.Osifchin, R.P. Andres and R. Reifenberger, Phys. Rev B **52**, 9071 (1995)
5 U. Banin, Y.-W. Cao, D. Katz and O. Millo, Nature **400**, 542 (1999).
6 E.P.A.M. Bakkers and D. Vanmaekelbergh, Phys. Rev. B **62**, R7743 (2000).
7 D. Vanmaekelbergh, E.P.A.M. Bakkers, A. Franceschetti, A.Zunger, L.Gurevich, L.Canali, M. Janus and L.P. Kouwenhoven, submitted to Nanoletters.
8 L. Gurevich, L. Canali and L.P. Kouwenhoven, Appl. Phys. Lett. **76**, 384 (2000)
9 D.L. Klein, R. Roth, A.K.L. Lim, A.P. Alivisatos and P.L. McEuen, Nature **389**, 699 (1997)
10 A. Bezryadin, C. Dekker, G. Schmid Appl. Phys. Lett. **71**, 1273 (1997)
11 H.Park, J.Park, A.K.L. Lim, E.H. Anderson, A.P. Alivisatos, P.L. McEuen, Nature **407**, 57 (2000)
12 D.C. Ralph, C.T. Black and M. Tinkham, Phys. Rev. Lett. **74**, 3241 (1995)
13 C.B. Murray, D.J. Norris and M.G. Bawendi, J. Am. Chem. Soc. **115**, 8706 (1993).
14 J. W. G. Wildöer, A.J.A. van Roy, H. van Kempen, and C. J. P. M. Harmans, Rev. Sci. Instrum. **65**, 2849 (1994).
15 L.P. Kouwenhoven, C.M. Markus, P.L. McEuen, S. Tarucha, R.M. Westervelt, and N.S. Wingreen, in Proceedings of the NATO Advanced Study Institute on Mesoscopic Electron Transport, edited by L.L. Sohn, L.P. Kouwenhoven, and G. Schön (Kluwer Series E345, 1997) p. 105-214
16 The gold colloids (mean diameter of 20.1 nm, range 18.5 - 22.5 nm) were bought from Research Diagnostics Inc
17 K.K. Likharev, IEEE Transactions on Magnetics, **MAG-23**, 1142 (1987).